

A Study On the Zn(II) Separation Efficiency of Chemically Synthesized Hydroxyapatite (HAp) Particles

Ahmet Dizle¹, Yağmur Uysal^{2*}

¹Institute of Science, Kahramanmaraş Sütçü İmam University, Avşar Kampüsü, 46000, Kahramanmaraş, Turkey

²Department of Environmental Engineering, Faculty of Engineering, Mersin University, Mersin 31343, Turkey

•Received Date: Apr 2, 2021

•Revised Date: May 20, 2021

•Accepted Date: June 09, 2021

•Published Online: Jun 24, 2021

Abstract

In this study, hydroxyapatite particles (HAp) were chemically synthesized by using co-precipitation method to determine their capabilities on the sorption of Zn(II) ions from aqueous solutions. HAp particles were chosen because of their low cost for production, high stability, easy to use, and effective sorption power. In order to determine the operation conditions of the adsorption system to be installed when this adsorbent is desired to be used in field applications, parameters such as system pH, initial Zn(II) concentration and adsorbent concentrations have been optimized. Properties and functional structure of the adsorbent materials were characterized by using SEM, FTIR, and EDX analyzes. The kinetic behavior of Zn(II) adsorption with HAp was consistent with the pseudo second order kinetic model. Additionally, the equilibrium states of the adsorption processes were studied by using Langmuir, Freundlich, Temkin, Scatchard and Dubinin–Radushkevich (D-R) isotherm models. The maximum sorption capacity HAp was obtained as 500 mg/g, and best removal value of 91% were determined at pH of 6.0, optimum adsorbent concentration of 3.75 g/L, in 25 mg/L Zn(II) concentration and optimum mixing time of 45 min. This study showed that the HAp can be considered an effective adsorbent on the Zn(II) removal from wastewater.

Keywords

Adsorption, Hydroxyapatite, HAp, Removal, Zn(II)

*Corresponding Author: Yagmur Uysal, yuyisal@mersin.edu.tr,  [0000-0002-7217-8217](https://orcid.org/0000-0002-7217-8217)

1. INTRODUCTION

Heavy metals such as Zn(II), Cd(II), Cr(VI), and Pb(II) etc. have toxic properties, so they are harmful to all livings. Many industrial wastewater contains these ions in different concentrations, so they must be removed from the discharges before reach to the receiving environments. High concentrations of Zn(II) have been observed in wastewaters from pharmaceutical, galvanizing, paint, pigment, insecticide, cosmetic industries, and leachate of landfills [1, 2]. Many treatment techniques have been used to remove these trace ions from water and wastewater such as adsorption, chemical precipitation, filtration, complexing, and electrochemical treatment. The most important parameters before choosing the most appropriate treatment methods for an application should be economy and sustainability of the used technique when considering large volumes of wastewaters. Adsorption is an effective, speed and economical method wastewater treatment applications when adsorbents used in have high sorption capacities [3]. In recent years, researchers have been moving towards producing and using innovative adsorbents such as hydroxyapatite, polymeric materials and biomass [4, 5]. For example, Çelebi et al. [6] investigated the heavy metal removal efficiency of some brewed tea wastes (*Camellia sinensis*) from simulated watery solution. They found that optimum pH as 4.0-5.0 to remove Pb, Zn, Ni, Cd ions from water by adsorption method. The authors emphasized that when using the brewed tea wastes in the adsorption process, the equilibrium values were reached in a short time (2, 10, 30 and 5 minutes, respectively) in the removal of Pb, Zn, Ni and Cd, and that the tea wastes had the potential to be used in the removal of heavy metals. Using tea wastes, maximum adsorption capacities were obtained for Pb, Zn, Ni and Cd as 1.197, 1.457, 1.163 and 2.468 mg/g, respectively.

Similarly, eggshell powder (ESP) has been tried as an inexpensive adsorbent material to remove different heavy metals from water by adsorption method. The highest Cd(II) removal efficiency was found at pH 5.0, an initial ESP dosage of 3.5 g, temperature at 20 °C, agitation speed at 250 rpm and contact time of 60 minutes. The maximum removal efficiency of ESP for Cd(II) ions was obtained between 65% and 96% under optimum conditions (pH 5.0, 3.5 g ESP and 60 min) and the maximum adsorption capacity was 2.221 mg/g [7].

Recently, nanometer-sized adsorbents such as iron oxide-based materials with superparamagnetic characteristics have been commonly used as adsorbents due to their low toxicity, ease of synthesis and economic compared to commonly used adsorbents [8, 9]. Nano-adsorbents can be used in the environmental purification techniques because of their high sorption capacity within a short time [10, 11].

The apatites are natural calcium phosphate mineral which can be extracted from soil, used in agriculture, in bone tissue and in nature. In most of the studies conducted in recent years, hydroxyapatite (HAp) ($\text{Ca}_5(\text{PO}_4)_3(\text{OH})$), which has porous structure and is presented in the structure of natural bones, teeth, eggshells and also shells of some animals, is used as natural adsorbent for water purification. In addition, its production is easier and uncomplicated than other adsorbents for practical applications than other adsorption materials such as biochar, clays [12], and nanotubes and zeolites [13, 14]. There are many studies using HAp as a natural adsorbent material to remove several metal ions. For example, adsorption potential of HAp for Pb(II), Cd(II), Zn(II), Sr(II) ions were studied and quite high removal efficiencies were obtained in literature [15-17]. In addition, it was also reported that phosphate content in the HAp provided immobilization of metal ions, and a dissolution–precipitation mechanism of metal phosphates contributed the metal removal [18].

In this study, Zn(II) adsorption capacity of hydroxyapatite particles prepared by co-precipitation method was investigated. The experimental factors affecting the process such as pH, reaction time, and concentration of Zn(II) were determined. In order to find rate of the adsorption of Zn(II) ions, kinetic studies were also made, and kinetic and isotherm models that best describe the research results were explained.

2. MATERIALS AND METHODS

2.1. Chemicals

All chemicals used in this research such as $\text{Ca}(\text{NO}_3)_2 \cdot 4\text{H}_2\text{O}$, $(\text{NH}_4)_2\text{HPO}_4$, NH_4OH (25%) were analytical grade (purchased from Merck). Zn(II) stock solutions were prepared from ZnCl_2 . pH adjustments were made by using 0.1 M HCl (37%) and 0.1 M NaOH solutions (Merck).

2.2. Synthesis of HAp Particles

HAPs were prepared with according to Wang et al. [19] from $\text{Ca}(\text{NO}_3)_2 \cdot 4\text{H}_2\text{O}$ (0.4 M) and $(\text{NH}_4)_2\text{HPO}_4$ (0.16 M). First, a homogeneous mixture of $(\text{NH}_4)_2\text{HPO}_4$ (0.16 M) and $\text{Ca}(\text{NO}_3)_2 \cdot 4\text{H}_2\text{O}$ (0.4 M) was prepared. $(\text{NH}_4)_2\text{HPO}_4$ solution was mixed up to 60°C by using magnetic stirrer, and added to the $\text{Ca}(\text{NO}_3)_2 \cdot 4\text{H}_2\text{O}$ solution at 60°C. White color was observed during this addition. 5 M NH_4OH solution was added until the pH of the mixture was 10. It was then stirred at 60°C for 3 hours. The mixture was left for 24 h at room temperature. The white precipitate formed was washed with ultrapure water until it reached to neutral pH. Then it was separated from the liquid phase with the help of centrifuge, and dried at 80°C. As a result of these experimental sequences, adsorbent material was obtained and the calculated reaction

efficiency was found to be 80%. The precipitates of HAp were isolated by centrifugation and washed with pure water to reach neutral pH. Then precipitates were dried at 80 °C overnight to obtain the HAp adsorbent.

2.3. Adsorbent Characterization

Particle sizes and their morphology of synthesized HAp particles were characterized by a Scanning Electron Microscope (SEM- ZEISS/EVO LS10 Model). The characterization of the adsorbents was analyzed by FTIR (Fourier Transform Infrared Spectrophotometer-Perkin Elmer Spectrum 400 Model), and Energy Dispersive X-Ray Analysis (EDX-ZEISS/EVO LS10 Model) for elemental analysis. The pH measurements were made by pH-meter (Hanna HI 2211 pH/ORP). ICP-OES (Optima 2100-Perkin Elmer) was used to determine Zn(II) concentrations in water.

2.4. Experiments

The pH effect on Zn(II) removal was studied by mixing 6.25 g/L HAp with 25 mg/L Zn(II) containing solutions. The pH was adjusted to pH 2.0-9.0 range. Because of the metal hydroxide precipitation occurred at pH>8.5, the maximum pH value was chosen as pH 9.0. Experiments were conducted at different HAp dosages of 1.25-12.5 g/L with constant pH (optimum) and 25 mg/L Zn(II) concentration to find optimum adsorbent concentration. Similarly, different Zn(II) concentrations of 10-100 mg/L, and different reaction times of 5-180 min experiments were conducted at to find optimal conditions. According to the water pollution control regulation, the receiving environment discharge standard for industries such as metal, mining, chemical, textile and petroleum industry that discharges wastewater containing zinc ions varies from 3-12 mg/L. For this reason, 10-100 mg/L was chosen for the initial concentration range for zinc ions in our study and to include the high range. The kinetic behavior of Zn(II) adsorption on MHAp was studied by measuring its residual concentrations with time intervals. The Zn(II) uptake capacity, q (mg/g) was examined based on the Eq. 1;

$$q = \frac{C_0 - C_e}{M} \quad (1)$$

C_0 and C_e ; Zn(II) concentrations at the beginning of the experiments and at equilibrium after adsorption (mg/L), V ; solution volume (L), and M ; mass of the HAp (g/L).

2.5. Kinetic Experiments

Adsorption kinetics refer to the time dependence of the adsorption process. The most commonly used equations developed for the purpose of explaining the adsorption kinetics are first degree, pseudo second degree and intraparticle diffusion. The first-order kinetic model introduced by

Lagergren has been applied for the initial stages in which the adsorption process has not yet reached its equilibrium. This equation is as follows (Eq 2) [20].

$$\frac{dq}{dt} = k_1(q_e - q_t) \quad (2)$$

After the integration, equation is converted to formula below, Eq. 3.

$$\log(q_e - q_t) = \log(q_e) - \frac{k_1}{2.303} t \quad (3)$$

In this equation, q_e and q_t show the adsorbate amount on the adsorbent at equilibrium and at any time of t . k_1 is rate constant (1/min). The equation of the second order kinetic model, which is in harmony with the speed control mechanism throughout the adsorption period, is as follows (Eq. 4) [21].

$$\frac{t}{q_t} = \frac{1}{k_2 q_e^2} + \frac{t}{q_e} \quad (4)$$

k_2 shows the rate constant (g/mg.min), and it is calculated from the slope and intercept values. This model provides to design and find size of the adsorption reactor for pilot scale and real applications.

Intraparticle diffusion model (Weber-Morris) was developed to define an inexplicable adsorption model with first and second degree models [22] (Eq. 5);

$$q_e = k_p t^{0.5} \quad (5)$$

where; k_p is intra-particle diffusion model rate constant for (mg/g 1/2); $t^{0.5}$: half time (min); C : equilibrium ratio constant for intra-particle diffusion model.

2.6. Adsorption Isotherms

The equilibrium data of adsorption processes were analyzed using the Langmuir (Eq. 6), Freundlich (Eq. 7), Dubinin Radushkevich (D-R) (Eqs. 9-10), Tempkin (Eqs. 11-12), and Scatchard (Eq. 13) adsorption isotherm models:

$$\frac{1}{q_e} = \frac{1}{b q_m C_e} + \frac{1}{q_m} \quad (6)$$

$$\ln q_e = \ln K_f + \frac{1}{n \ln C_e} \quad (7)$$

where, q_e (mg/g) is HAp capacity for Zn(II) adsorption, C_e is Zn(II) concentration in equilibrium (mg/L), q_m is maximum capacity of HAp for Zn(II) adsorption (mg/g), K_F and K_L are the coefficients of Freundlich and Langmuir models, and n is the exponent of Freundlich model.

Freundlich and Langmuir isotherms are commonly used isotherms to explain the relationship between adsorbent and adsorbate in the removal of various contaminants from water. The

Langmuir isotherm model is used to express the monolayer surface adsorption of contaminants to a limited number of binding points on the adsorbent surface. Freundlich isotherm states that the bonding is not in the form of a single layer on the surface, but bonding occurs by overlapping more than one layer. The interaction of metal ions and biosorbents was further examined by separation factor (R_L). R_L equals to a dimensionless constant separation factor, as an equilibrium parameter derived from the Langmuir model. The R_L was described by Hall et al. [23] and was shown in Eq. (8). R_L values imply that the isotherm is favorable ($0 < R_L < 1$), unfavorable ($R_L > 1$), linear ($R = 1$), or irreversible ($R = 0$).

$$R_L = \frac{1}{1+bC_0} \quad (8)$$

Dubinin Radushkevich (D-R) isotherm gives information about the porosity of the system. The basis of the isotherm equation is based on the micropore volume distribution [24]. As the adsorption energy decreases, the capacity of the adsorbate to fill the pores on the adsorbent is increased.

$$\varepsilon = RT \ln \left(1 + \frac{1}{C_e} \right) \quad (9)$$

$$\ln q_e = \ln Q_s - B\varepsilon^2 \quad (10)$$

Where; Q_s : Maximum adsorption capacity of HAp for Zn(II) adsorption (mg/g); B: D-R isotherm constant; ε : Polanyi adsorption potential (kJ/mol); R: Universal gas constant (8.3144 J/°K.mol); T: Temperature (°K)

Interactions between the adsorbed substances are taken into account in the Tempkin isotherm. This isotherm was developed according to the adsorption enthalpy of all molecules in solution, and assumes that heat of adsorption of all the molecules in the layer decreases linearly with coverage due to adsorbent–adsorbate interactions [25, 26].

$$q_e = B \ln A_T + B \ln C_e \quad (11)$$

$$B = \frac{RT}{b_t} \quad (12)$$

b_t : Temkin isotherm constant (J/mol); A_T : Equilibrium binding constant (L/g); T: Temperature (°K)

Scatchard isotherm can give more reliable results than Langmuir and Freundlich isotherm equations when it is used for the characterization of various materials, and characteristics of the adsorbate material. In other words, it is possible to comment on the suitability of the Langmuir and Freundlich models from the Scatchard curve derived for an adsorption process.

$$\frac{q_e}{C_e} = Q_s K_s - q_e K_s \quad (13)$$

where; Q_s : Maximum adsorption capacity of HAp for Zn(II) adsorption (mg/g), and K_s : Binding constant

3. RESULTS AND DISCUSSION

3.1. Characterizations Of The Adsorbents

The structural properties of the adsorbent used in the adsorption process are important factors affecting the adsorption rate and efficiency. The surface area, particle size and structure of the adsorbent are factors affecting the adsorption efficiency. Increasing of surface area and decreasing of particle size affect all adsorption processes positively. In the present study, FTIR analyzes were made to determine the chemical characterization of adsorbent before and after the adsorption as below (Fig. 1).

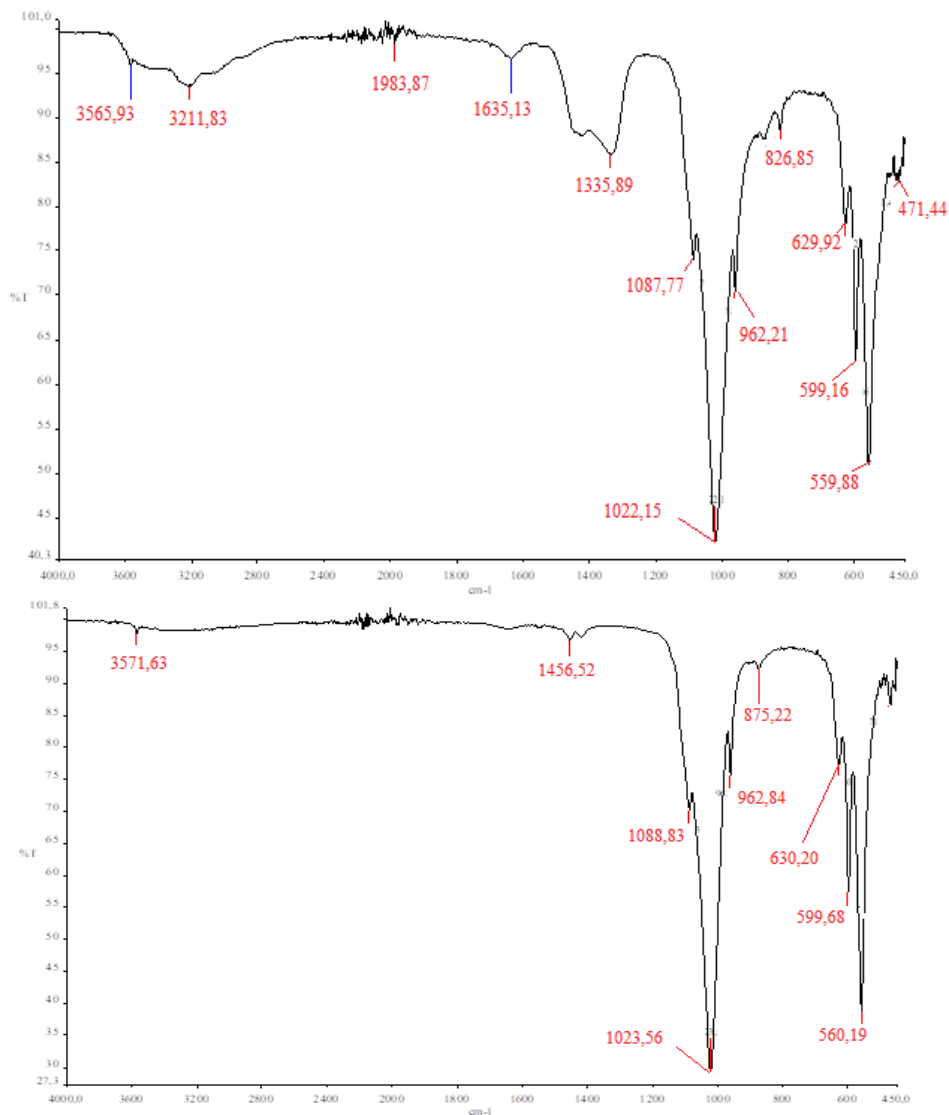


Figure 1. FTIR analyzes before (a) and after (b) the adsorption process of the HAp

In the FTIR spectrum, the signaling of the oxygen-hydrogen (O-H) bonds was observed in the 3565 cm^{-1} and 3571 cm^{-1} regions. The peaks at 1635 , and 1022 - 1023 cm^{-1} correspond the C=C and C=O stretching [27]. The peaks in the 599 cm^{-1} and in the 560 cm^{-1} regions are considered to the low phosphate stretch zone (tensile vibrations of PO_4^{3-} in the HAp) [28]. The peaks in

the area of $1335\sim 1456\text{ cm}^{-1}$ are considered to belong to the high phosphate stretch region. Adsorption occurs as a result of displacement of Ca^{+2} and Zn^{+2} ions in 1456 and 1335 cm^{-1} band [29]. The FTIR spectrum confirmed that the hydroxyapatite contains oxygenated functional groups. Since all these groups are available adsorption zones, they have a great role in heavy metal removal [30]. The results also showed that there were changes in the location and intensity of peaks after the adsorption. It was interpreted that peaks at $3565\text{-}3211\text{ cm}^{-1}$, $1635\text{-}1335\text{ cm}^{-1}$ regions were relatively lost after adsorption, and zinc could be bounded to the bonds in these regions. Therefore, it is concluded that the adsorption of zinc ions to the surface of the adsorbents is chemical.

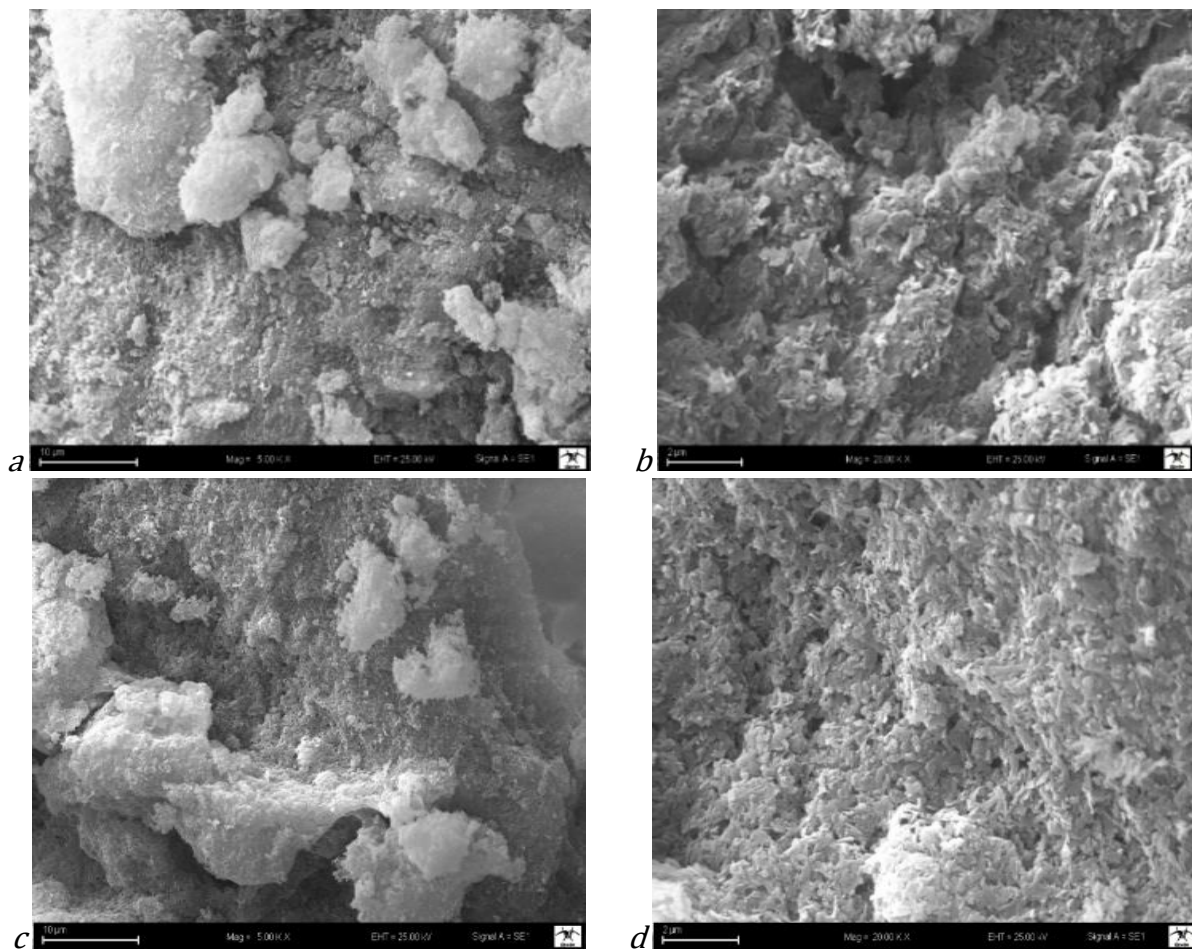


Figure 2. SEM surface analyses of hydroxyapatite particles before (a,b) and after (c,d) the adsorption process

SEM surface analyses of the adsorbent were investigated before and after the treatment process, and the following images were obtained (Fig. 2). The results showed that the adsorbent is generally composed of fine and spherical particles and has an irregular and porous structure. Therefore, these pores on the surface of the adsorbent can explain their effectiveness in the removing of metal ions. When the post-adsorption results were examined, it was shown that this porous and hollow structure is less than before and the adsorption is successful. After the

adsorption, it was determined that the pores and cavities on the adsorbent surfaces were closed and the pores were closer to each other.

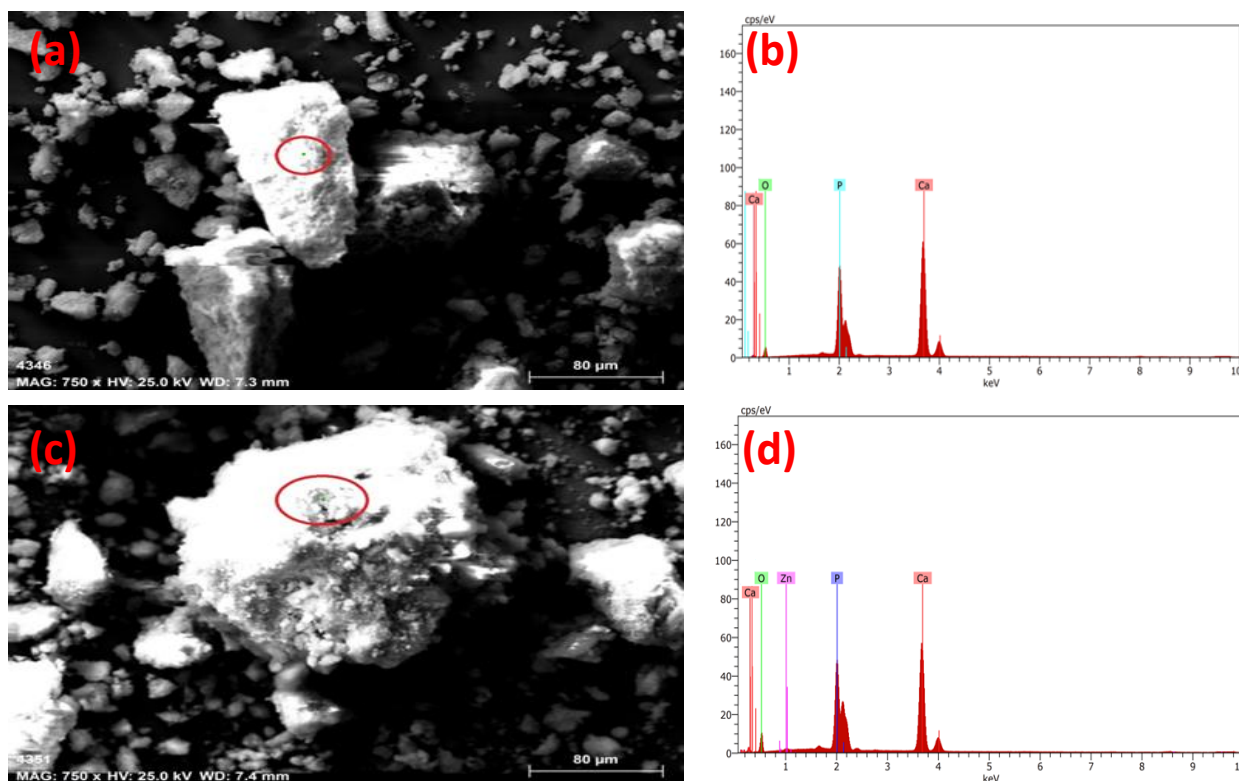


Figure 3. EDX analysis of HAp particles before (a, b) and after (c, d) the adsorption

The data obtained from the EDX elemental analyses of the adsorbent are shown in Fig. 3. In the EDX analyses carried out at one point of the adsorbent, the presence of elements in the structure of the adsorbent appears before the adsorption. The presence of zinc in addition to the elements in the adsorbent structure in the post-adsorption EDX analysis showed that Zn (II) ions were successfully adsorbed on the HAp surface.

Elemental analysis of pure hydroxyapatite showed that it contains 56.02% Calcium (Ca), 22.28% Oxygen (O) and 21.70% Phosphorus (P) in its mass. After the adsorption process, its EDX analysis showed that it contains 42.14% Ca, 24.84% O, 21.72% P, and 11.28% Zn(II) in its mass. The presence of the Zn(II) ions indicates the Zn(II) adsorption of hydroxyapatite. Moreover, the reason for the decrease in calcium concentration after contact can be explained by the replacement of Zn (II) ions with Ca (II) ions on the surface.

3.2. Experiments

3.2.1. The change of Zn(II) adsorption by HAp with pH

The pH effects the solubility/precipitation conditions, mobility of metal ions, and also surface properties of the adsorbents. In addition, solution pH is important as it affects the surface charge of the adsorbent and the availability of metal ions in aqueous solution as free metal ions [31].

Thus, solution pH affects the adsorption of metal ions on adsorbent surface directly. In order to investigate the effect of different initial pH on adsorption process, HAp particles (6.25 g/L) were added to the flasks containing 10 and 25 mg/L of Zn(II) solutions at different initial pH (2.0-9.0), and batch adsorption tests were made at room temperature (23 °C) for 60 minutes (Fig. 4).

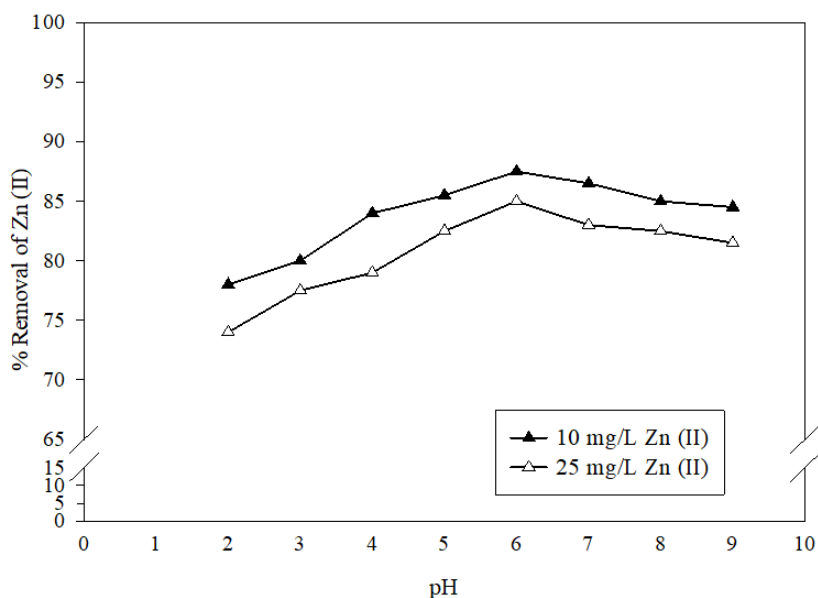


Figure 4. The change of Zn(II) removal by pH (HAp: 6.25 g/L, t: 60 min)

As seen in the Fig. 4, solution pH has a strong effect on the Zn(II) adsorption by HAp and the percentage of adsorbed Zn(II) increased with the increase of the solution pH up to 6.0. Removal efficiencies for HAp at pH 2.0-9.0 range were found in the range of 78.0-87.5% and 74.0-85.0% for 10 and 25 mgZn(II)/L, respectively. An increase in the adsorption efficiency was observed at pH values of 2.0-6.0. In order to the decrease in the density of the positive charges on the solid surfaces with the increase of pH, also decrease of competition between the Zn(II) and H^+ ions for active adsorbent sites, the removal efficiency of Zn(II) decreased with higher pH values as a result of the decrease of electrostatic forces and precipitation of metal ions with the hydroxide in the solution. Thus, pH 6.0 was selected as the optimal pH value because of closing to neutral pH, avoiding to surface protonation at lower pHs, and to precipitation of Zn(II) ions at high pHs. Thus, pH for Zn(II) adsorption was fixed at 6.0 in the next adsorption experiments. Thanh et al. [32] used the magnetite-hydroxyapatite nanocomposite for the removal of Cu (II) and nickel Ni (II) ions from the solutions. In order to determine the effect of pH on the adsorption process, they tried different pH ranges of 3.0-5.0 and 3.0-7.0, and they found optimum pH values for Cu (II) and Ni (II) as 5.0 and 7.0, respectively. Similarly, Nahid et al. [33] used magnetite amino nanoparticles as adsorbent for Zn(II) removal. They carried out the experiments at different initial pH range of 2.0-7.0, initial Zn(II) concentration of 5-20 mg/L,

adsorbent dosages of 0.005-0.040 g/25 mL, adsorption time of 5-120 min, and temperature of 308-333 °K range. They reached the best Zn(II) removal at pH range of 6.0-8.0.

These results are similar to those obtained in previous studies on the adsorption behavior of Zn (II) on various adsorbent materials such as mixed column clays [34]; geopolymeric Linz-Donawitz powder [35] and hydrous manganese dioxide [36]. Thanh et al. [32] reported that four mechanisms such as complex formation, ion exchange, dissolution-precipitation and electrostatic interaction on the adsorbent surface are effective on metal retention by magnetite composite and raw hydroxyapatite adsorbents. Other mechanisms such as surface sorption and complexation were suggested by other researches for metal ions at high pH values (>4.0) [37].

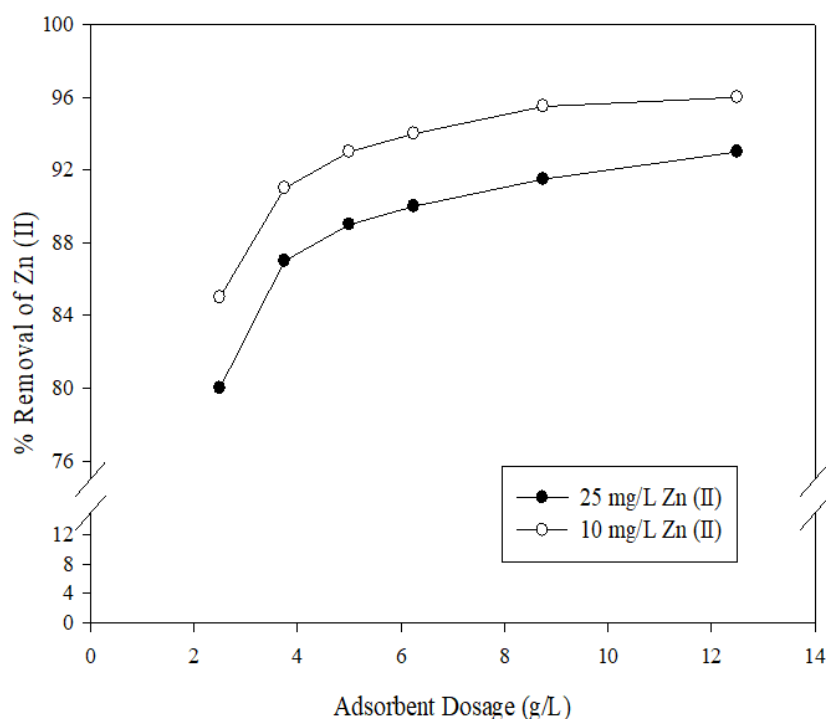


Figure 5. The change of Zn(II) removal by HAp dosage (HAp: 2.5-12.5 g/L; t: 60 min, pH:6.0)

3.2.1. The change of Zn(II) adsorption by HAp with HAp concentration

In the adsorption process, reaction rate changes with the amount of adsorbate added to the solution. Since the amount of adsorbate per unit volume will vary at different concentrations, adsorbate amount adsorbed by the adsorbent will also change, and affects the adsorption efficiency depending on the adsorbent capability and capacity. Thus, experiments were made at room temperature (22 ± 1 °C) for 60 min by using the amount of adsorbents in the range of 1.25-12.5 g/L at pH 6.0 (Fig. 5). As seen in Fig. 5, the increase of adsorbent concentration caused to increase of Zn(II) removal efficiency for two different Zn(II) concentrations. Increasing of binding sites for Zn(II) with the presence of high adsorbent addition lead to

increase of active sites on their surface, so this caused to increase of Zn(II) removal efficiencies. The maximum removal efficiency of 96% was obtained at the maximum HAp concentration of 12.5 g/L while, this value was found as 91% for 3.75 g/L adsorbent concentration. The active surface area and the number of pores on the adsorbent surface increase with increasing of adsorbent concentration, so much more Zn(II) ions can be further adsorbed on them. In the results shown in Fig 5, the peak in the removal rate was observed at 3.75 g/L adsorbent concentration, and there was an only 5% yield difference between 12.5 g/L and 3.75 g/L adsorbent concentrations for both Zn(II) concentrations. Thus, optimum adsorbent concentration for HAp particles was chosen as 3.75 g/L to avoid the use of much amount adsorbent considering of economic factors.

Harja and Ciobanu [38] used HAp as adsorbent material to remove oxytetracycline (OTC) from wastewater, and found that OTC removal showed an increase with increasing of adsorbent concentration with surface complexation mechanism. They pointed out that adsorption success of adsorbents increases by increasing of their surface area and related active sites. Periyasamy et al. [39] used hydroxyapatite alginate beads (1-4 g/L) to remove Cr(VI) (100-200 mg/L) from water, and they determined optimum adsorbent concentration as 4 g/L for these experimental conditions.

Wang et al. [19] also worked on hydroxyapatite-biochar nanocomposite (HAp-BC) to remove metal ions such as lead, zinc and copper, and they reported that when the solution pH is too acidic (pH <2.5), heavy metal adsorption can be negatively affected by the adsorbent surface being positively charged.

3.2.2. The change of Zn(II) adsorption by concentration and time

Heavy metals are commonly found in industrial wastewater, and different metal ions can be found in these wastewaters in different concentrations depending on the type of water and industry. Therefore, the initial concentration of heavy metal ions to be removed in adsorption studies is a factor affecting the process efficiency. In our study, Zn(II) concentration effect (10-100 mg/L) on adsorption was determined by keeping the other parameters constant (pH:6.0, HAp: 3.75 g/L, t: 60 min, T: 22±2°C).

The adsorbed Zn(II) concentration decreased with increasing of initial Zn(II) concentration because of their active sites were constant (Fig. 6). In the lowest Zn(II) concentration of 10 mg/L, the removal efficiency of HAp was measured as 88%. However, it was decided to choose optimum initial concentration of Zn(II) as 25 mg/L because of reaching to quite high removal efficiency of 85 %.

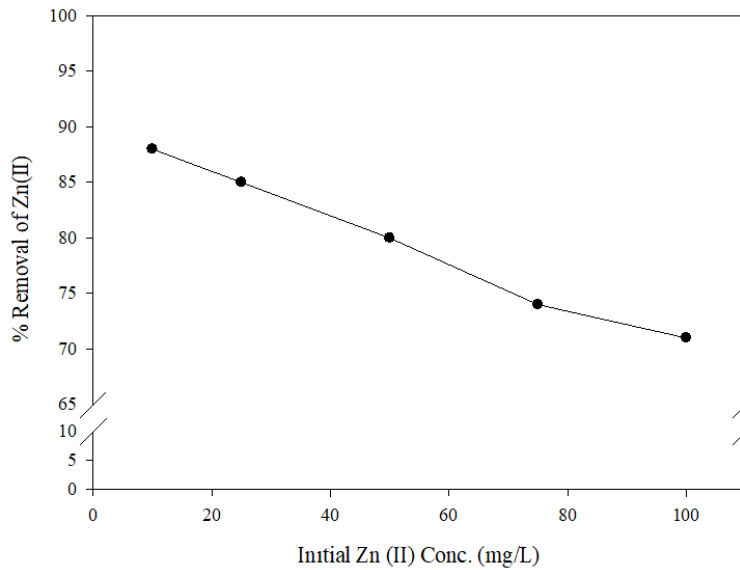


Figure 6. The change of Zn(II) removal by initial Zn(II) concentration (HAp: 3.75 g/L, t: 60 min, pH:6.0, 10-100 mg/L)

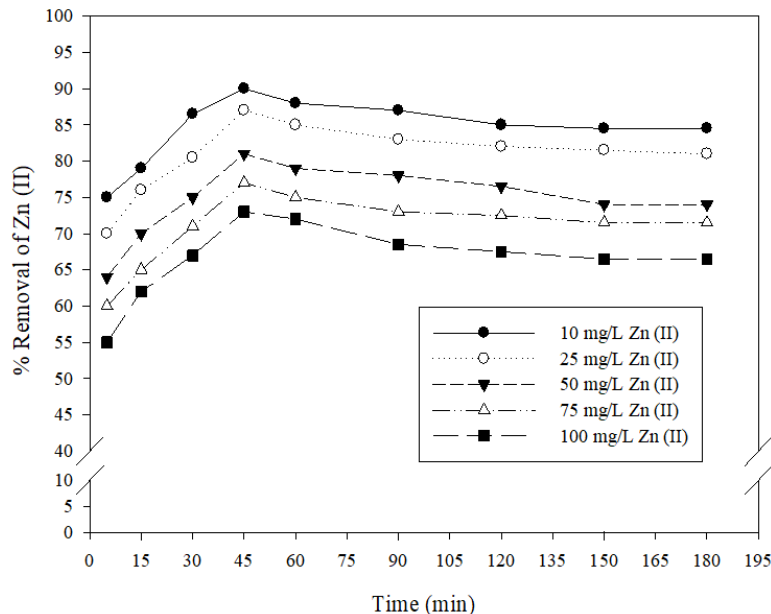


Figure 7. Effect of reaction time on Zn(II) removal (HAp: 3.75 g/L, pH:6.0, 10-100 mgZn(II)/L, t: 5-180 min)

In the adsorption process, a certain time is required to adhere the adsorbate to the adsorbent surface. Thus, one of the most important criteria to be determined in the applications of the adsorption is to determine the optimum contact time. Adsorption efficiency will increase with increasing of the contact time up to a certain period, and it will reach to stable value after the reach to equilibrium. In order to determine the effect of contact time on the adsorption, experiments were conducted keeping all other parameters constant (pH 6.0, HAp: 3.75 g/L, and 10-100 mgZn(II)/L) for 5-180 min. According to Fig. 7, the removal efficiency reached the maximum in the first 45 min for HAp particles. Although removal efficiencies reduced slightly after reaching to their maximum values, they did not change significantly over time after from

90 min. 73-90% of zinc ion adsorption occurred at the first 45 min for HAp particles depending on the initial Zn(II) concentration levels. This is due to the high level of unsaturated active sites of adsorbents at the start of contact time. In the experiments, in order to determine whether the adsorbent added to the solutions causes changes in the pH of the water and the effect of these pH changes on heavy metal removal, the pH measurements of all the initial Zn (II) concentrations in the contact time experiment were made and shown in Fig. 8.

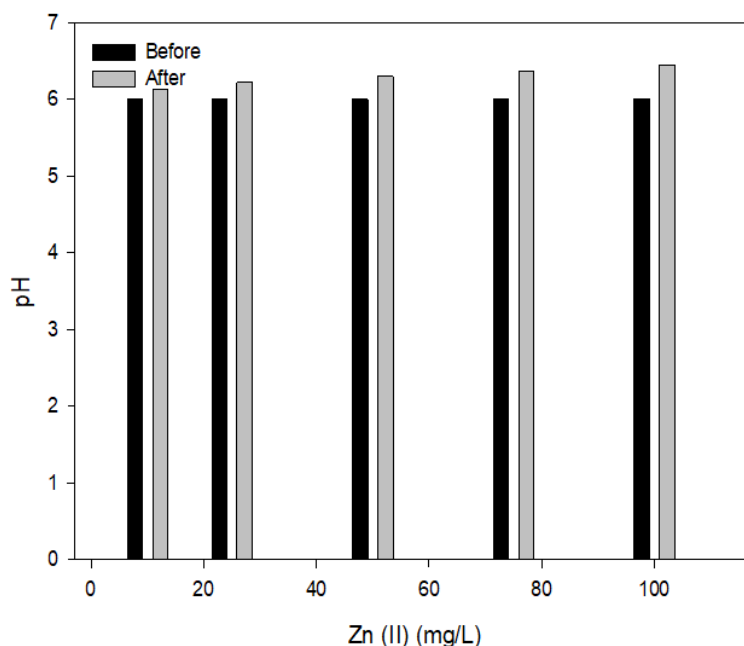


Figure 8. Solution pHs before and after adsorption according to the initial Zn (II) concentrations

3.3. Adsorption Kinetics

Kinetic experiments are performed to identify and understand the functions that control the adsorption mechanisms such as chemical and/or physical reaction and diffusion. With this aim, time-adsorption capacity results were applied to different kinetic models to find kinetic behavior of Zn(II) adsorption (Fig. 9), and adsorbent/adsorbate relationships were determined between Zn(II) and HAp particles (Table 1). The first degree equation was not well suited for describing the kinetic behavior of the Zn(II) adsorption. However, the pseudo-second degree equation with R^2 value of 0.9992 for HAp was found to be best kinetic equation describing Zn(II) adsorption kinetic on hydroxyapatite powders followed by the diffusion-controlled process which is the intraparticle (pore) diffusion model (R^2 -HAp:0.9643). The results showed that not only the surface adhesion or surface chemistry is effective on the adsorption rate but also closely related to the pore structure of the hydroxyapatite at the micro or macro level. The results also showed that in the adsorption process, firstly, Zn (II) ions were rapidly transported to the surface of the adsorbents and then diffused into the particles [39].

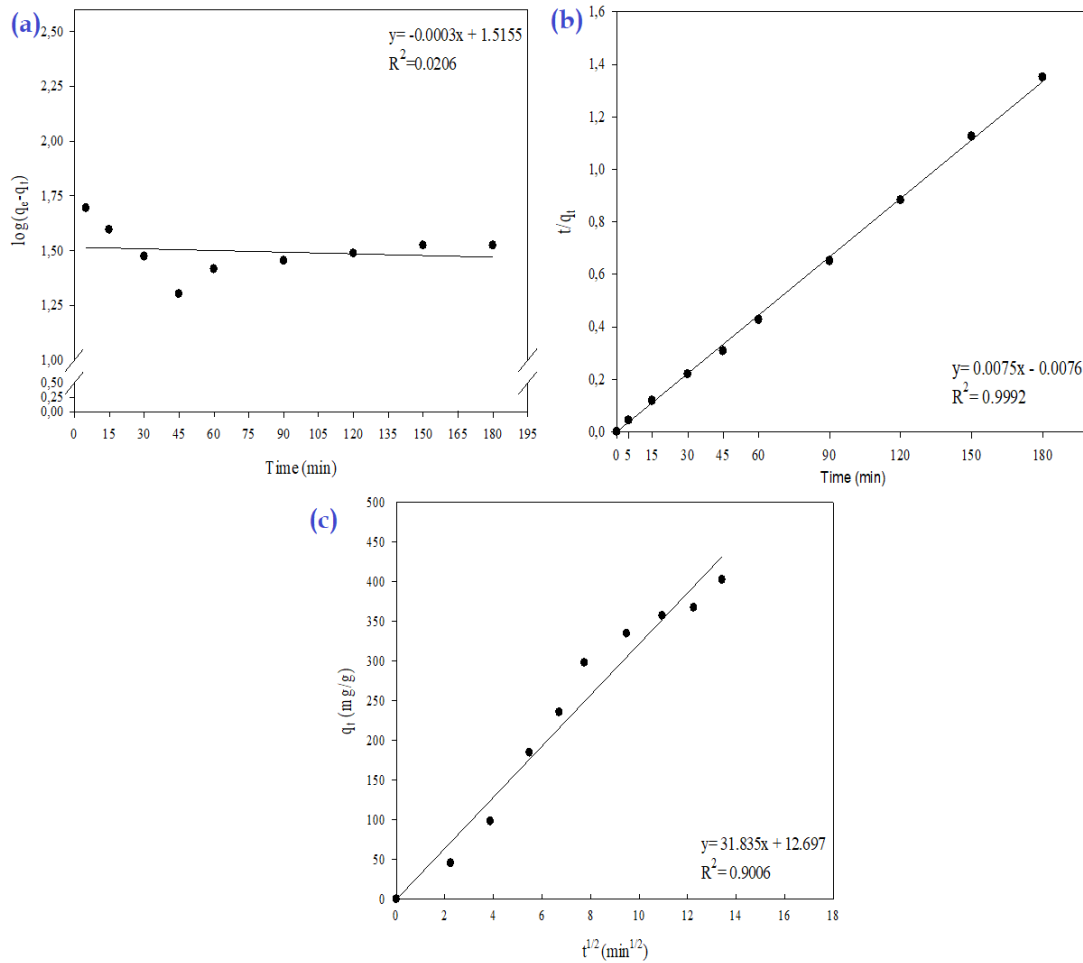


Figure 9. The first degree (a), pseudo-second degree (b) and intraparticle diffusion (c) models for Zn(II) removal by HAp

Table 1. Kinetic behavior of HAp for Zn(II) removal (pH 6.0, 3.75 g/L, 25 mgZn(II)/L, 22±2 °C)

Kinetic models	Parameters	Value
First degree kinetic $\log(q_e - q_t) = \log q_e - (k_1/2.303)t$	$q_{e,calc}$ (mg/g)	32.770
	k_1 (min^{-1})	0.0007
	R^2	0.020
	SS	0.002
	MS	0.002
	P	0.712
Pseudo-second degree kinetic $t/q_t = (1/k_2 q_e^2) + (1/q_e)t$	$q_{e,calc}$ (mg/g)	133.333
	k_2 (g/mg.min)	0.007
	R^2	0.999
	SS	4.629
	MS	0.463
	P	<0.0001
Intraparticle diffusion kinetic $q_t = k_p t^{0.5} + C$	C	12.697
	k_{id} (mg/g·min ^{0.5})	31.835
	R^2	0.900
	SS	726721
	MS	72672
	P	<0.0001

SS: Sum of Squares; MS: Mean Squares; Results are statistically significant ($p < 0.05$).

3.4 Adsorption Isotherms

In the adsorption processes, removal of the material from the solution continue until an equilibrium to be form between the adsorbent and adsorbate. The adsorption isotherm studies reveal the interaction between adsorbent and adsorbate when adsorption reaches equilibrium and show the maximum adsorption capacity of the adsorbent. In other words, the results of the isotherm studies are applied on the selection and to determine the potential efficiency of the adsorbent to be used before the results are put into practice in real scale. Process feasibility can be assessed for a given application by using experimental isotherms for example the most suitable adsorbent or the adsorbent dosage requirements can be determined. The regression coefficients of the four isotherm models used, and the parameters required to show the which isotherm is compatible are given in Table 2.

The correlation coefficients (R^2) for Freundlich and Langmuir models were found to be higher than the correlation coefficients of the other models. Both Freundlich and Langmuir models explained the isotherm behavior of adsorbent very well. Based on R^2 values, Freundlich model (R^2 : 0.9909) described the Zn(II) adsorption on HAp very well, implying that the adsorption process involved multi-molecular layers of coverage. Specifically, the $1/n$ value (0.623) indicating that the adsorbent has relatively more homogeneous binding sites. However, the Langmuir model was found to be more consistent with the experimental results with correlation coefficient R^2 of 0.9978. The separation factor (R_L) was found to be between 0 and 1 (0.227), and this value indicated to be a favorable sorption process for HAp. The Langmuir model shows that binding sites of adsorbent have an equal affinity for the adsorbate, and adsorption occurred with the formation of a monolayer by homogenous adsorbent sites. The results showed that Zn (II) ions perform monolayer coating on adsorbent surfaces and adsorption is homogeneous. The maximum Zn(II) adsorption capacities obtained by unit adsorbent mass were calculated from Langmuir model as 500 mg/g.

Table 2. Isotherm parameters for Zn(II) adsorption on HAp

Isotherms	Parameters			
	R^2	B (L/mg)	q_m (mg/g)	R_L
Langmuir	0.9993	0.136	500	0.227
	R^2	K_f (mg/g)	$1/n$	
Freundlich	0.9909	65.45	0.623	
	R^2	B_T	A_T (L/mg)	
Tempkin	0.9595	125.59	1.27	
	R^2	K_s	Q_s	
Scatchard	0.9387	0.101	623.08	
	R^2	B	Q_s	E
Dubinin Radushkevich	0.8479	2.979	331.98	2.44

4. CONCLUSIONS

In this study, hydroxyapatite powders were prepared by wet co-precipitation method, and the batch adsorption experiments were performed to determine Zn(II) removal potential of them. Adsorption reactions were dependent on pH, HAp amount, and contact time and initial Zn(II) concentration. After the adsorption reaction started, it happened rapidly and reached its maximum value in the first 45 minutes. While the optimum adsorbent concentration was 3.75 g/L, the adsorption efficiency was obtained as 90%. Thus, HAp exhibited excellent adsorption performance for Zn(II) as a novel adsorbent with maximum adsorption capacity of 500 mg/g. The kinetic behavior of HAp adapted to pseudo-second degree kinetic and pore diffusion models very well, and isotherm results could be explained by Langmuir and Freundlich isotherms. The results showed that hydroxyapatite particles obtained from natural sources or chemically synthesized can be a new alternative adsorbent for removing zinc ions from wastewater in treatment applications.

REFERENCES

- [1] H.J. Fan, H.Y. Shu, H.S. Yang, W.C. Chen, *Characteristics of landfill leachates in Central Taiwan*, *Sci. Total Environ.* 361 (2006) 25–37.
- [2] A.K. Bhattacharya, S.N. Mandal, S.K. Das, *Adsorption of Zn(II) from aqueous solution by using different adsorbents*, *Chem. Eng. J.* 123 (2006) 43–51.
- [3] M.N. Rashed, *Adsorption technique for the removal of organic pollutants from water and wastewater*, INTECH Open Access Publisher, 2013 167-194.
- [4] G. Crini, *Non-conventional low-cost adsorbents for dye removal: a review*, *Bioresource Technol.* 97 (2006)1061–1085.
- [5] J.L. Gong, B. Wang, G.M. Zeng, C.P. Yang, C.G. Niu, Q.Y. Niu, W.J. Zhou, Y. Liang, *Removal of cationic dyes from aqueous solution using magnetic multi-wall carbon nanotube nanocomposite as adsorbent*, *J. Hazard. Mater.* 164 (2009)1517–1522.
- [6] H. Çelebi, G. Gök, O. Gök, *Adsorption capability of brewed tea waste in waters containing toxic lead(II), cadmium (II), nickel (II), and zinc(II) heavy metal ions*, *Scientific Reports* 10, (2020) 17570.
- [7] S. Ozcan, H. Celebi, Z. Ozcan, *Removal of heavy metals from simulated water by using eggshell powder*, *Desalination and Water Treatment* 127 (2018) 75-82.
- [8] G. Liu, J. Gao, H. Ai, X. Chen, *Applications and potential toxicity of magnetic iron oxide nanoparticles*, *Small* 9 (2013) 1533-1545.
- [9] S. Bao, L. Tang, K. Li, P. Ning, J. Peng, H. Guo, T. Zhu, Y. Liu, *Highly selective removal of Zn(II) ion from hot-dip galvanizing pickling waste with amino-functionalized Fe₃O₄@SiO₂ magnetic nano-adsorbent*, *J. Colloid Interf. Sci.* 462 (2016) 235–242.

- [10] H. Karami, *Heavy metal removal from water by magnetite nanorods*, Chem. Eng. J. 219 (2013) 209–216.
- [11] M. Nagpal, R. Kakkar, *Use of metal oxides for the adsorptive removal of toxic organic pollutants*, Sep. Purif. Technol. 211 (2019) 522–539.
- [12] J.I. Yoo, T. Shinagawa, J.P. Wood, W.P. Linak, D.A. Santoianni, C.J. King, J.O.L. Wendt, *High-temperature sorption of cesium and strontium on dispersed kaolinite powders*, Environ. Sci. Technol. 39 (2005) 5087-5094.
- [13] T. Wen, X. Wu, M. Liu, Z. Xing, X. Wang, A.W. Xu, *Efficient capture of strontium from aqueous solutions using graphene oxide-hydroxyapatite nanocomposites*, Dalton Trans. 43 (2014) 7464-7472.
- [14] D. Yang, S. Sarina, H. Zhu, H. Liu, Z. Zheng, M. Xie, S.V. Smith, S. Komarneni, *Capture of radioactive cesium and iodide ions from water by using titanate nanofibers and nanotubes*, Angew Chem. Int. Ed. Engl. 50 (2011) 10594-10598.
- [15] N. Gupta, A.K. Kushwaha, M.C. Chattopadhyaya, *Adsorptive removal of Pb²⁺, Co²⁺ and Ni²⁺ by hydroxyapatite/chitosan composite from aqueous solution*, J. Taiwan Inst. Chem Eng 43(1) (2012) 125-131.
- [16] I. Smiciklas, S. Dimovic, I. Plecas, M. Mitric, *Removal of Co²⁺ from aqueous solutions by hydroxyapatite*, Water Res. 40 (2006) 2267-2274.
- [17] X. Xia, J. Shen, F. Cao, C. Wang, M. Tang, Q. Zhang, S. Wei, *A facile synthesis of hydroxyapatite for effective removal strontium ion*, J Hazard. Mater. 364 (2019) 326-335.
- [18] S. Sugiyama, T. Ichii, F. Masayoshi, K. Kawashiro, T. Tomida, N. Shigemoto, H. Hayashi, *Heavy metal immobilization in aqueous solution using calcium phosphate and calcium hydrogen phosphates*, J Colloid Interface Sci. 259 (2003) 408-410.
- [19] Y. Wang, Y. Liu, H. Lu, R. Yang, S. Yang, *Competitive adsorption of Pb(II), Cu(II), and Zn(II) ions onto hydroxyapatite-biochar nanocomposite in aqueous solutions*, J Solid State Chem. 261 (2018) 53–61.
- [20] S. Lagergren, *About the theory of so-called adsorption of soluble substances*, Kungliga Svenska Vetenskapsakademiens, Handlingar, Band 24, 1898, 1-39.
- [21] Y.S. Ho, G. McKay, *Pseudo-second order model for sorption processes*, Process Biochem. 34 (1999) 451-465.
- [22] W.J. Jr Weber, J.C. Morriss, *Kinetics of adsorption on carbon from solution*, J. Sanit. Eng. Div. 89 (1963) 31–60.
- [23] K.R. Hall, L.C. Eagleton, A. Acrivos, T. Vermeulen, *Pore and solid diffusion kinetics in fixed-bed adsorption under constant-pattern conditions*, Ind. Eng. Chem. Fundam., 5 (1966) 212–223.
- [24] T. Jiun-Horng, C. Hsiu-Mei, H. Guan-Yinag, C. Hung-Lung, *Adsorption characteristics of acetone, chloroform and acetonitrile on sludge-derived adsorbent, commercial granular activated carbon and activated carbon fibers*, J Hazard Mater. 154 (2008) 1183-1191.
- [25] M. Ghasemi, S. Mashhadi, M. Asif, I. Tyagi, S. Agarwal, V.K. Gupta, *Microwave-assisted synthesis of tetraethylenepentamine functionalized activated carbon with high adsorption capacity for Malachite green dye*, J. Mol. Liq. 213 (2016) 317-325.

- [26] S. Mashhadi, R. Sohrabi, H. Javadian, M. Ghasemi, I. Tyagi, S. Agarwal, V.K. Gupta, *Rapid removal of Hg (II) from aqueous solution by rice straw activated carbon prepared by microwave assisted H₂SO₄ activation: kinetic, isotherm and thermodynamic studies*, J. Mol. Liq. 215 (2016) 144-153.
- [27] C. Qi, Q.L. Tang, Y.J. Zhu, X.Y. Zhao, F. Chen, *Microwave-assisted hydrothermal rapid synthesis of hydroxyapatite nanowires using adenosine 5'-triphosphate disodium salt as phosphorus source*, Materials Letters, 85 (2012) 71-73.
- [28] G.N. Kousalya, R.M. Gandhi, C. Sairam Sundaran, S. Meenakshi, *Synthesis of nano-hydroxyapatite chitin/chitosan hybrid biocomposites for the removal of Fe(III)*, Carbohydr. Polym. 82 (2010) 594-599.
- [29] Y. Li, S. Wang, Y. Zhang, R. Han, W. Wei, *Enhanced tetracycline adsorption onto hydroxyapatite by Fe(III) incorporation*, J. Mol. Liq. 247 (2017) 171-181.
- [30] W. Yaoguang, H. Lihua, Z. Guangya, Y. Tao, Y. Liangguo, W. Qin, D. Bin, *Removal of Pb(II) and methylene blue from aqueous solution by magnetic hydroxyapatite-immobilized oxidized multi-walled carbon nanotubes*, J. Colloid Interface Sci. 494 (2017) 380-388.
- [31] A. Vahdat, B. Ghasemi, M. Yousefpour, *Synthesis of hydroxyapatite and hydroxyapatite/Fe₃O₄ nanocomposite for removal of heavy metals*, Environ. Nanotechnol. Monit. Manage 12 (2019) 100233.
- [32] D.N. Thanh, M. Singh, P. Ulbrich, F. Štěpánek, N. Strnadová, *As(V) removal from aqueous media using α -MnO₂ nanorods-impregnated laterite composite adsorbents*, Mater. Res. Bull. 47 (2012) 42-50.
- [33] G. Nahid, G. Maryam, M. Saleh, G. Paris, S.A. Njud, K.G. Vinod, S. Agarwal, I.V. Burakova, AV Tkachev, *Zn (II) removal by amino-functionalized magnetic nanoparticles: kinetics, isotherm, and thermodynamic aspects of adsorption*, J. Ind. Eng. Chem. 62 (2018) 302-310.
- [34] M.G. Saida, N. Frini-Srasra, *A comparison of single and mixed pillared clays for zinc and chromium cations removal*, Appl. Clay. Sci. 158 (2018) 150-157.
- [35] S. Chayan, K. Jayanta, A. Basu, S. Nath, *Synthesis of mesoporous geopolymeric powder from LD slag as superior adsorbent for zinc (II) removal*, Adv. Powder Technol. 29 (2018) 1142-1152.
- [36] S.B. Kanungo, S.S. Tripathy, Rajeev, *Adsorption of Co, Ni, Cu, and Zn on hydrous manganese dioxide from complex electrolyte solutions resembling sea water in major ion content*, J. Colloid Interface Sci. 269 (2004) 1-10.
- [37] E. Valsami-Jones, K.V. Ragnarsdottir, A. Putnis, D. Bosbach, A.J. Kemp, G. Cressey, *The dissolution of apatite in the presence of aqueous metal cations at pH 2-7*, Chem. Geol. 151 (1998) 215-233.
- [38] M. Harja, G. Ciobanu, *Studies on adsorption of oxytetracycline from aqueous solutions onto hydroxyapatite*, Sci. Total Environ. 628-629 (2018) 36-43.
- [39] S. Periyasamy, V. Gopalakannan, N. Viswanathan, *Hydrothermal assisted magnetic nano-hydroxyapatite encapsulated alginate beads for efficient Cr(VI) uptake from water*, J. Environ. Chem. Eng. 6 (2018) 1443-1454.